Energy Conversion and Management 51 (2010) 2913–2920

Contents lists available at ScienceDirect

Energy Conversion and Management

journal homepage: www.elsevier.com/locate/enconman

Preliminary design of seawater and brackish water reverse osmosis desalination systems driven by low-temperature solar organic Rankine cycles (ORC)

Agustín M. Delgado-Torres [a,*], Lourdes García-Rodríguez [b]

[a] Dpto. Física Fundamental y Experimental, Electrónica y Sistemas, Escuela Técnica Superior de Ingeniería Civil e Industrial, Universidad de La Laguna (ULL), Avda. Astrofísico Francisco Sánchez s/n. 38206 La Laguna (Tenerife), Spain

[b] Dpto. Ingeniería Energética, Universidad de Sevilla Escuela Técnica Superior de Ingenieros, Camino de los Descubrimientos, s/n 41092 Sevilla, Spain

ARTICLE INFO

Article history:
Received 16 January 2009
Received in revised form 6 October 2009
Accepted 7 June 2010

Keywords:
Solar organic Rankine cycle
Solar ORC
Solar reverse osmosis
Solar desalination

ABSTRACT

In this paper, the coupling between the low-temperature solar organic Rankine cycle (ORC) and seawater and brackish water reverse osmosis desalination units has been carried out. Four substances have been considered as working fluids of the solar cycle (butane, isopentane, R245fa and R245ca). With these four fluids the volumetric flow of fresh water produced per unit of aperture area of stationary solar collector has been calculated. The former has been made with the optimized direct vapour generation (DVG) configuration and heat transfer fluid (HTF) configuration of the solar ORC. In the first one (DVG), working fluid of the ORC is directly heated inside the absorber of the solar collector. In the second one (HTF), a fluid different than the working fluid of the ORC (water in this paper) is heated without phase change inside the absorber of the solar collector. Once this fluid has been heated it is carried towards a heat exchanger where it is cooled. Thermal energy delivered in this cooling process is transferred to the working fluid of the ORC. Influence of condensation temperature of the ORC and regeneration's process effectiveness over productivity of the system has also been analysed. Finally, parameters of several preliminary designs of the low-temperature solar thermal driven RO desalination are supplied. R245fa is chosen as working fluid of the ORC in these preliminary designs. The information of the proposed preliminary designs can also be used, i.e., for the assessment of the use of thermal energy rejected by the solar cycle. Overall analysis of the efficiency of the solar thermal driven RO desalination technology is given with the results presented in this paper and the results obtained with the medium temperature solar thermal RO desalination system presented by the authors in previous papers. This work has been carried out within the framework of the OSMOSOL and POWERSOL projects.

1. Introduction

OSMOSOL project [1] is a Spanish government-funded project for the technological development of the solar thermal driven reverse osmosis (RO) desalination. Among the specific objectives of the project, the preliminary design of solar desalination systems of capacities between 100 m^3/day and 1000 m^3/day was proposed where a solar thermal heated organic Rankine cycle drives the high pressure pump of the RO unit. Besides that, in the POWERSOL project [2], development of a small scale shaft power generation technology (50–500 kW) for electricity generation and fresh water production by brackish water or seawater reverse osmosis desalination is being carried out. Solar thermal driven RO desalination is a renewable energy driven desalination technology that has not been studied in depth neither from a theoretical (e. g. design proposals) nor experimental point of view, as it was concluded from the specific bibliographic review already done and published by the authors [3,4] and confirmed by Ghermandi and Messalem [5] in a subsequent review work about status of solar driven (thermal and photovoltaic) RO desalination. As for experimental systems, only one of the five that can be quoted has been built in the twenty-one century, being the rest built at the end of the seventies (1978) and in the eighties (1981 and 1987). The reason for the scarcity of systems of this type could be the high values of the specific energy consumption that RO desalination process exhibited around that time, what made the solar thermal energy-driving of the RO process non-viable. In fact, the four old systems were brackish water RO desalination systems which have lower specific energy consumption than seawater RO systems. The only solar thermal driven RO experimental system erected at the moment is the system developed in the Agricultural University of Athens [6]. Results of the whole system operation under real solar conditions have been published by Manolakos et al. [7] and also

* Corresponding author. Tel.: +34 922318102; fax: +34 922318228.
E-mail address: amdelga@ull.es (A.M. Delgado-Torres).

0196-8904/$ - see front matter © 2010 Elsevier Ltd. All rights reserved.
doi:10.1016/j.enconman.2010.06.032

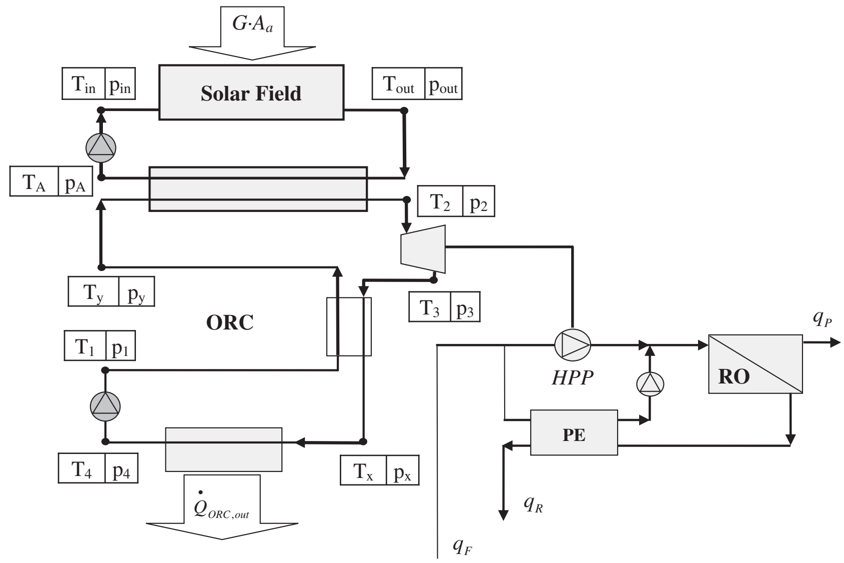

Fig. 1. Basic layout of the low-temperature solar thermal driven reverse osmosis desalination system in a heat transfer fluid configuration of the solar cycle.

the performance results of the organic Rankine engine and the small RO unit under laboratory conditions (electrical heating) have been given [8,9].

Solar thermal driven water pumping systems follow a similar operation principle than solar thermal RO desalination systems. Comprehensive bibliographic review of these systems has been already made and published by the first author [3,10]. It showed that in solar thermal water pumping systems based on conventional thermodynamic methods the Rankine cycle with organic fluids has been the most used power cycle.

As for solar thermal RO desalination, the authors have made the detailed analysis of the coupling between the solar organic Rankine cycle (ORC) with parabolic trough collectors and a seawater reverse osmosis unit [11,12]. However, the assessment of the low-temperature solar thermal reverse osmosis desalination is also an interesting issue because ORC technology is a promising technology to exploit low temperature heat sources [13] and only the works of Manolakos et al. [6,8] about de design of the experimental system, Kosmadakis et al. [14,15] and Bruno et al. [16] can be cited in this field. Kosmadakis et al. [15] present a simulation of a double cascade solar ORC for RO desalination to estimate the increase in the efficiency and the energy available for desalination due to the use of an upper ORC coupled with a lower ORC with R134a as used in the experimental system [7]. The working fluid selected for the upper cycle of the saturated ORC would be the R245fa with a maximum temperature of 137 °C whereas the condensation temperature of the lower cycle with R134a would be 35 °C. However, a single ORC with R245fa as working fluid would have higher efficiency than the proposed double cascade system operating between the same two extreme temperatures and the condensation pressure would be higher that ambient pressure too because the normal boiling point of the fluid (15.1 °C). Lower cost of the single ORC unit would be expected and, for a fixed RO unit, higher efficiency of the ORC would cause a smaller solar field needed. Finally the cost of the system and the fresh water produced would be lower. In other words, the double cascade ORC could not be the right option for low-temperature solar thermal energy exploitation. Bruno et al. [16] also present yearly simulations of a low and medium temperature solar ORC-RO system without thermal energy storage and thermal energy backup which implies partial load operation of pumps and especially of vapour turbine, whose efficiency is a key parameter for the thermal efficiency of the ORC unit (thermal efficiency of the ORC is nearly proportional to the isentropic efficiency of the expander).

In the system under study (see heat transfer fluid configuration in Fig. 1), the higher the efficiency of the solar energy to mechanical energy conversion, the higher the volumetric flow rate of desalted water per unit of aperture area of the solar field: this is the main objective of the optimization process. Therefore, the first step of the analysis of low-temperature solar RO system was the optimization of the low-temperature solar organic Rankine cycle [17] taking the overall efficiency of the power cycle as objective function. Four organic substances (isobutane, isopentane, R245ca and R245fa) were finally selected as working fluids of the ORC. In the present, paper the results of the coupling of these solar power cycles with these four fluids with brackish water and seawater reverse osmosis units are presented. As in the medium temperature analysis [11,12,18] quotient between volumetric flow rate of desalted water and aperture area of the solar field (unit volumetric flow rate) is considered as the most representative parameter of the system because it reflects the effect of the solar collector's efficiency, ORC's thermal efficiency and specific energy consumption of the RO unit. These are the main factors that determine the performance of the overall system. Influence of other parameters as condensation temperature and effectiveness of the regenerator on unit volumetric flow rate is also studied. Results obtained can not be checked with any other theoretical study because no similar one has been found in the specific literature. Comparison with the unique experimental system can not be done either because the preliminary design presented in this paper correspond to a RO desalination capacity around 1000 m^3/day whereas the performance results presented by [7] are about a small RO system of 0.3 m^3/h of capacity.

Table 1
Coefficients of the efficiency curve of solar collectors considered.

Solar collector[19]	η_{0a}	a_{1a} (W/m^2)	a_{2a} (W/m^2 K^2)
CPC Aosol 1.12X	0.736	4.61	0
VITOSOL 200F	0.791	3.94	0.0122
SchücoSol U.5 DG	0.793	2.92	0.0131
VITOSOL 300	0.730	1.26	0.0041

Table 2
Critical parameters, normal boiling point, molecular weight, TLV-TWA, autoignition temperature and global warming potential of each substance considered as working fluids of the solar Rankine cycle with stationary solar collectors.

Fluid	T_c (°C)	p_c (kPa)	T_{NBP} (°C)	M (g/mol)	EOS reference	TLV-TWA (ppm)	Autoignition temp. (°C)	$GWP_{100\ years}$
Isobutane	134.66	3629.0	−11.75	58.122	[20]	1000 [21]	460 [22]	<10 [23]
R245fa	154.01	3651.0	15.14	134.045	[24]	Not established	412 [25]	1030 [26]
R245ca	174.42	3925.0	25.15	134.050	[27,28]	Not established	Not established	693 [26]
Isopentane	187.20	3378.0	27.83	72.149	[24]	600 [22]	420 [22]	∼20 [29]

T_c ≡ critical temperature; p_c ≡ critical pressure; T_{NBP} ≡ normal boiling point temperature; M ≡ molecular weight; EOS ≡ equation of state; TLV ≡ threshold limit value; TWA ≡ time weighted average; GWP ≡ global warming potential.

The analysis presented here joint the bibliographic reviews [4,5,10] and medium temperature results [11,12] give an overview of this not very studied solar desalination technology.

2. Low-temperature solar thermal-driven RO desalination system

2.1. Stationary solar collectors

Stationary solar collector models considered in this paper are the same used in the detailed analysis of the low-temperature solar ORC [17]: a compound parabolic collector, two flat plate collectors and an evacuated tube collector. Coefficients of the certified efficiency curve of each collector model are given in Table 1.

2.2. Working fluids of the solar ORC

Substances considered in this paper as working fluids of the low-temperature solar ORC are presented in Table 2. These fluids were selected after a detailed analysis based on several criteria: solar power cycle efficiency, safety, toxicity and environmental impact of the fluids and size of equipment [17].

Heat rejection pressure in the ORC is above atmospheric pressure for a fixed condensation temperature of 30 °C with all the fluids considered according with their values of the normal boiling point (see Table 2). This fact would avoid vacuum operation in the condenser unit of the ORC.

The slope of the saturated vapour entropy line in the *T–s* diagram is one of the main advantages of using organic substances as working fluids of the Rankine cycle [30]. Many of these fluids have a positive or almost infinite value of this slope as can be observed in Fig. 2. This property means that there is no condensation inside the vapour turbine during the expansion process of the ORC and has some influence on the relative importance of regeneration process.

Saturation pressure is another thermodynamic property of the substance that has to be into account in its assessment as working fluid of the ORC. Saturation pressure curves of fluids are shown in Fig. 3. Heating pressures would be lower than 3.5 MPa whatever the fluid used if a maximum saturation temperature of 150 °C is considered for the low-temperature cycle.

Finally, safety and environmental properties of the fluid should be analysed within the selection process. Some values of indicative parameters are given in Table 2 where, as can be observed, the selected fluids are non-ozone depleting and their auto ignition temperatures are far from the highest values that could be reached by the fluid in the low-temperature solar ORC (<150 °C).

2.3. Reverse osmosis system

Seawater and brackish water reverse osmosis (RO) units have been designed in order to obtain the lowest possible value of the specific energy consumption of the RO core, complying with the design limits established by the membranes manufacturer. Therefore, high productivity membranes and pressure exchanger devices (PES) as energy recuperation systems have been considered just like in the medium temperature solar thermal desalination analysis [11,12] (see Fig. 1). For small and medium capacity RO systems, this type of energy recuperation device is more suitable than Pelton turbines. It is considered that the RO core is formed by n_p pressure vessels connected in parallel with n_m high productivity membrane elements connected in series inside. Values of input parameters of the dimensioning process are given in Table 3.

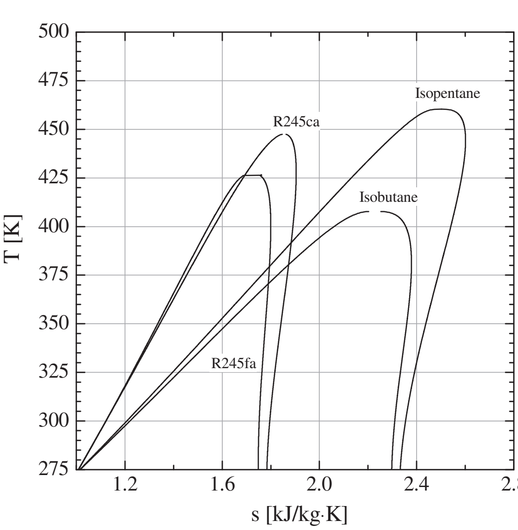

Fig. 2. Temperature-entropy diagrams of R245ca, R245fa, isobutane and isopentane.

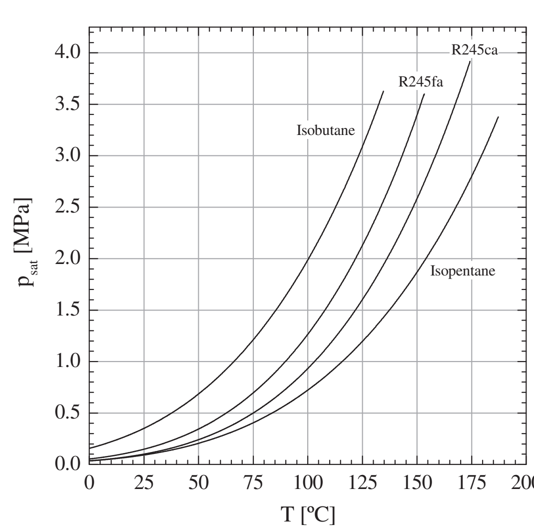

Fig. 3. Saturation pressure of R245ca, R245fa, isobutane and isopentane.

Table 3
Preliminary design parameters of reverse osmosis units.

	Sea water (SW)	Brackish water (BW)
Reverse osmosis membrane model	SWC5	CP3
GFD ($l\,h^{-1}\,m^{-2}$)	16 (<typical)	24 (<typical)
GFD of first element ($l\,h^{-1}\,m^{-2}$)	29.1 (<conservative)	32.8 (<conservative)
Pressure drop per vessel	100 kPa	100 kPa
Initial feed seawater pressure, permeate pressure and		
Concentrate's discharge pressure	100 kPa	100 kPa
Efficiency of high pressure pump, η_{HP}	0.85	0.85
Efficiency of booster pump, η_B	0.75	0.75
Feed water salinity	35,730 ppm	5331 ppm
Initial feed water temperature	20 °C	20 °C
Energy recovery system*	Pressure exchanger	Pressure exchanger
Conversion	45%	60%
Number of membranes per vessel (n_m)	7	7

* 200 kPa of pressure difference is assumed between blowdown input and feedwater output of pressure exchanger, which results in a pressure exchanger efficiency above 96%.

Table 4
Output values of the dimensioning process.

	Sea water (SW)	Brackish water (BW)
Fresh water salinity	225 ppm	49 ppm
Number of pressure vessels, n_p	10	7
High pressure	52.4 bar	16.2 bar
High pressure pump energy consumption (kW)	67.0 kW	20.4 kW
Volumetric flow rate of product	1001 m^3/day	1049 m^3/day

As can be observed, values of the average permeate flux (GFD) of the system and permeate flux of the first membrane element of the pressure vessel labelled as typical and conservative respectively by membrane manufacturer, were used in the dimensioning process. Values of output parameters for the seawater and brackish water RO units of freshwater capacity production around 1000 m^3/day are given in Table 4. Detailed analysis of the dimensioning process can be found in [3,11].

2.4. Coupling between solar ORC and RO unit

Coupling between solar ORC and RO desalination unit is carried out assuming that the net mechanical power delivered by the solar ORC ($\dot{W}_{net}$) is consumed by the high pressure pump of the RO core. This is the same approach followed in the medium temperature analysis [11]. Therefore:

$$\left|\dot{W}_{net}\right| = \frac{\dot{W}_{HPP}}{\eta_m} \quad (1)$$

where $\dot{W}_{HPP}$ is the mechanical power consumed by the high pressure pump (HPP) of the RO unit and η_m is the mechanical efficiency of the direct coupling between said pump and the vapour turbine of the ORC. Neglecting kinematic and potential energy variations of the feedwater (*fw*) flow across the high pressure pump and assuming that its operation is adiabatic, $\dot{W}_{HPP}$ in Eq. (1) can be written as:

$$\dot{W}_{HPP} = \frac{\dot{m}_{fw,HPP} \cdot \Delta h_{s,fw,HPP}}{\eta_{HPP}} \quad (2)$$

where $\dot{m}_{fw,HPP}$ is the mass flow rate of feed water flowing across the high pressure pump, $\Delta h_{s,fw,HPP}$ is its isentropic enthalpy variation and η_{HPP} is the isentropic efficiency of the pump. Since RO feedwater can be considered as a low compressibility fluid, Eq. (2) can be given as a function of the volumetric flow rate of feedwater compressed by the high pressure pump ($q_{fw,HPP}$) and the pressure difference ($\Delta p_{fw,HPP}$):

$$\dot{W}_{HPP} \cong \frac{q_{fw,HPP} \cdot \Delta p_{fw,HPP}}{\eta_{HPP}} \quad (3)$$

Besides that, in a RO unit with pressure exchanger as energy recovery system (see Fig. 1), the volumetric flow rate of desalted water (q_P) is equal to the volumetric flow rate of feedwater compressed by the high pressure pump [31]:

$$q_{fw,HPP} = q_P \quad (4)$$

Therefore, coupling between solar ORC and RO unit (1) can be written as a function of the volumetric flow rate of desalted water and the pressure difference provided with the high pressure pump:

$$|\dot{W}_{net}| = \frac{q_P \cdot \Delta p_{fw,HPP}}{\eta_m \cdot \eta_{HPP}} \quad (5)$$

Since the efficiency of the solar ORC is defined as follows:

$$\eta = \frac{\left|\dot{W}_{net}\right|}{A_a \cdot G} \quad (6)$$

where A_a is the aperture area of the solar field, G is the solar irradiance on the aperture of the solar collector and therefore $A_a \cdot G$ is the solar power gathered by the solar field, with (5) and (6) the volumetric flow rate of fresh water per unit of aperture area is:

$$\overline{q_P} = \frac{q_P}{A_a} = \eta_m \cdot \eta_{HPP} \cdot G \cdot \frac{\eta}{\Delta p_{fw,HPP}} \quad (7)$$

Although Eq. (7) is user-friendly because only the pressure difference in the high pressure pump has to be calculated, in this work the low compressibility approximation is not used for an accurately calculus. In this case, the volumetric flow rate of desalted water per unit of aperture area would be, using Eq. (2):

$$\overline{q_P} = \frac{q_P}{A_a} = \eta_m \cdot \eta_{HPP} \cdot G \cdot \frac{\eta}{\rho_{fw} \cdot \Delta h_{s,fw,HPP}} \quad (8)$$

where ρ_{fw} is the density of the RO feedwater. Thermodynamic properties of sea salt solutions were calculated with the model developed by García-Rodríguez [32].

The RO-solar ORC coupling has been made for two different solar cycle configurations: (1) direct vapour generation (DVG) and (2) heat transfer fluid (HTF). In the first case, the working fluid of the ORC flows inside the absorber tubes of the solar collector and is directly heated with the thermal energy produced by the solar collector. In the second one, a fluid different from the ORC's working fluid is heated without phase change inside the absorber tubes (see Fig. 1). Once this fluid has been heated it is carried towards a heat exchanger where it is cooled. The thermal energy delivered in this cooling process is transferred to the working fluid of the ORC. Values of fixed parameters needed for the calculation of solar collector efficiency and optimized values of solar ORC effi-

Table 5
Values of fixed parameters for the optimization of the solar ORC and the coupling of this with the reverse osmosis units.

Condensation temperature, T_{cond}	30 °C
Pump's isentropic efficiency, η_p	0.75
Turbine's isentropic efficiency, η_t	0.75
Regenerator effectiveness, ε_{reg}	0.80
Mechanical efficiency of direct ORC–HPP coupling, η_m	0.95
Solar irradiance, G	1000 W/m^2
Ambient temperature, T_{amb}	25 °C

ciency (6) are given in Table 5. Details of the calculation procedure of η can be found in Delgado-Torres and García-Rodríguez [17].

3. Preliminary design of the low-temperature solar thermal – powered desalination system

3.1. Volumetric flow rate of fresh water per unit of aperture area

Once the energy coupling of solar ORC and RO unit is calculated, the quotient between desalted water volumetric flow rate (q_p) and the solar collector aperture area needed (A_a) is also considered in this work – like in the medium temperature analysis [11,12] – as the representative quantity for the analysis of said coupling. This quotient will be named here as unit volumetric flow rate of fresh water ($\overline{q_p}$). Values of this performance parameter obtained after the optimization of the solar regenerative ORC efficiency (6) assuming HTF configuration are given in Figs. 4 and 5 for seawater and brackish water RO, respectively. These values are given for each solar collector model and each fluid considered.

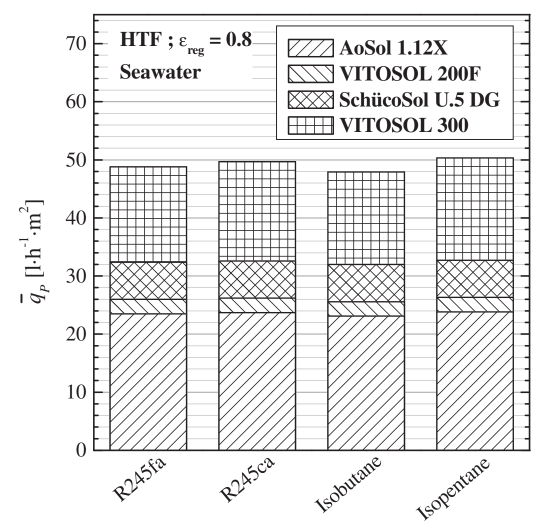

Fig. 4. Unit volumetric flow rate of desalted water as a function of working fluid and solar collector model for the seawater RO solar desalination system. Power cycle: HTF solar regenerative organic Rankine cycle. T_{cond} = 30 °C, G = 1000 W/m^2.

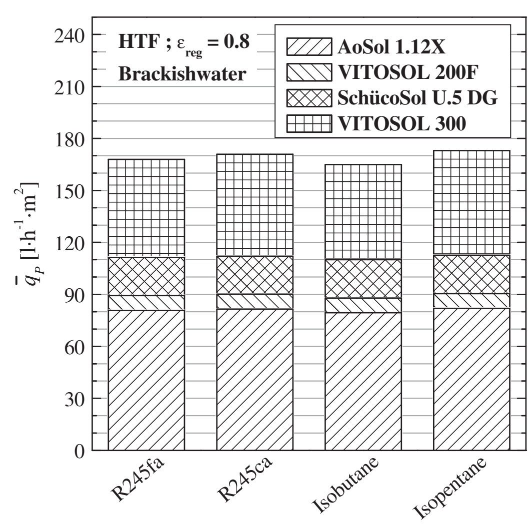

Fig. 5. Unit volumetric flow rate of desalted water as a function of working fluid and solar collector model for the brackish water RO solar desalination system. Power cycle: HTF solar regenerative organic Rankine cycle. T_{cond} = 30 °C, G = 1000 W/m^2.

As can be observed, isopentane is the fluid that yields the highest values of unit volumetric flow rate of fresh water straight on R245ca, R245fa and isobutene. This order does not depend on the solar collector model. In the case of the seawater RO system, values of $\overline{q_p}$ are about 23 l h^{-1} m^{-2} with CPC AoSol, 26 l h^{-1} m^{-2} with VITOSOL 200F, 32 l h^{-1} m^{-2} with FPC SchücoSol U.5 DG and 50 l h^{-1} m^{-2} with the ET VITOSOL 300. Values of $\overline{q_p}$ increase up to 81 l h^{-1} m^{-2}, 90 l h^{-1} m^{-2}, 111 l h^{-1} m^{-2} and 170 l h^{-1} m^{-2} with each solar collector, respectively for brackish water.

For each combination of solar ORC configuration (HTF or DVG), non-regenerative and regenerative ORC (ε_{reg} = 0, 0.8) and seawater and brackish water reverse osmosis unit, intervals of $\overline{q_p}$ values obtained with the four working fluids and the four solar collector models considered are given in Tables 6 and 7 for SW and BW reverse osmosis, respectively.

3.2. Influence of condensation temperature, regeneration process and solar cycle configuration

Results showed in previous section were calculated for fixed values of condensation temperature (30 °C) and regenerator effectiveness (0.8). Values of these two parameters have a great influence over the thermal efficiency of the ORC and over the average heating temperature of the fluid in the solar collector so finally the overall efficiency of the solar ORC and therefore the unit volumetric flow rate of fresh water is affected (8). In this section this influence over $\overline{q_p}$ is quantified when condensation temperature (T_{cond}) varies between 20 °C and 40 °C and regenerator effectiveness (ε_{reg}) varies between 0 (non-regenerative cycle) and 1. Unit volumetric flow rate of desalted water as a function of T_{cond} and ε_{reg} is presented in Figs. 6 and 7 for seawater and brackish water RO systems, respectively. Both figures correspond to the optimized HTF solar ORC configuration with R245fa as working fluid and VITOSOL 300 as solar collector. Fixed parameters used are the same as used in previous sections (see Tables 2–5). Preheating of the RO feed water with the heat rejected by the solar ORC was not considered.

Since unit volumetric flow rate isolines are almost parallel in both cases, effect of T_{cond} can be given by means of a constant slope value. In the case of seawater RO solar thermal desalination system the influence of condensation temperature is between 0.446 l h^{-1} m^{-2}/°C and 0.553 l h^{-1} m^{-2}/°C when T_{cond} is between 20 °C and 40 °C and ε_{reg} is between 0 and 1. In the case of brackish water RO system these values grow up to 1.536 l h^{-1} m^{-2}/°C and 1.905 l h^{-1} m^{-2}/°C.

Influence of solar cycle configuration over the unit volumetric flow rate of desalted water has been also analysed. Results for seawater and brackish water RO systems are shown in Figs. 8 and 9,

Table 6
Intervals of unit volumetric flow rate values of fresh water per unit of aperture area (l h^{-1} m^{-2}) obtained for the low-temperature solar thermal driven seawater reverse osmosis system with each solar ORC configuration and every solar collector model. G = 1000 W/m^2, T_{cond} = 30 °C.

	Seawater RO + solar ORC			
	DVG		HTF	
Regenerator effectiveness	ε_{reg} = 0	ε_{reg} = 0.8	ε_{reg} = 0	ε_{reg} = 0.8
Solar collector				
CPC Aosol 1.12X	[28.6–29.5]	[29.8–31.2]	[20.9–21.5]	[23.1–23.8]
FPC VITOSOL 200F	[31.5–32.5]	[33.0–34.3]	[23.1–23.8]	[25.6–26.3]
FPC SchücoSol U.5 DG	[36.6–37.5]	[38.8–40.1]	[28.1–28.9]	[32.0–32.7]
ETC VITOSOL 300	[46.3–51.5]	[53.0–57.5]	[41.2–42.7]	[47.9–50.3]

Table 7
Intervals of volumetric flow rate values of fresh water per unit of aperture area (l h^{-1} m^{-2}) obtained for the low-temperature solar thermal driven brackish water reverse osmosis system with each solar ORC configuration and every solar collector model. G = 1000 W/m^2, T_{cond} = 30 °C.

	Brackish water RO + solar ORC			
	DVG		HTF	
Regenerator effectiveness	ε_{reg} = 0	ε_{reg} = 0.8	ε_{reg} = 0	ε_{reg} = 0.8
Solar collector				
CPC Aosol 1.12X	[98.3–101.6]	[102.6–107.2]	[71.9–74.0]	[79.5–81.9]
FPC VITOSOL 200F	[108.3–111.7]	[113.5–117.9]	[79.5–81.9]	[88.0–90.5]
FPC SchücoSol U.5 DG	[125.8–129.0]	[133.3–137.8]	[96.8–99.5]	[110.1–112.5]
ETC VITOSOL 300	[159.2–177.3]	[182.2–197.6]	[141.7–147.0]	[164.9–173.0]

respectively. Both figures correspond to an ORC with R245fa as working fluid of the cycle.

As in the case of the working fluid used, influence of solar power cycle configuration does not depend on the solar collector model.

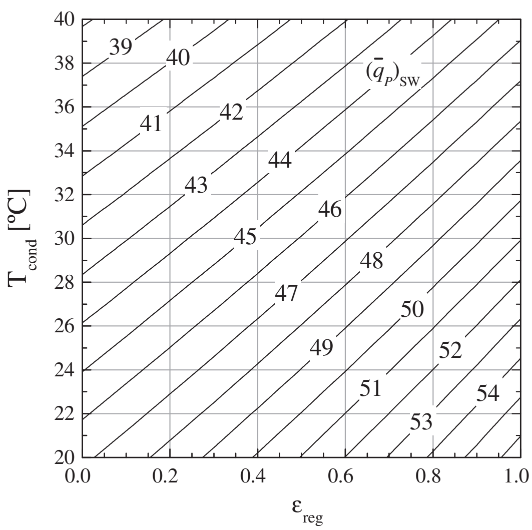

Fig. 6. Influence of condensation temperature and regeneration effectiveness over the unit volumetric flow rate of desalted water [l h^{-1} m^{-2}]. Solar HTF ORC with VITOSOL 300, R245fa as working fluid, and seawater at 20 °C as feedwater of RO unit.

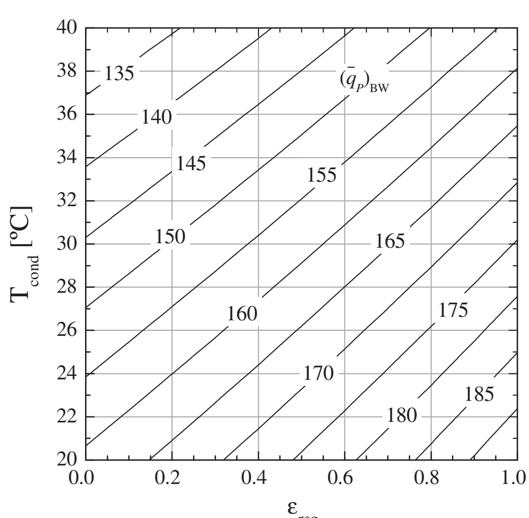

Fig. 7. Influence of condensation temperature and regeneration effectiveness over the unit volumetric flow rate of desalted water [l h^{-1} m^{-2}]. Solar HTF ORC with VITOSOL 300, R245fa as working fluid, and brackish water at 20 °C as feedwater of RO unit.

3.3. Parameters of the low-temperature solar thermal driven reverse osmosis desalination systems

Main parameters of the solar thermal driven reverse osmosis (RO) desalination system are given in Tables 8 and 9. These values are given for seawater and brackish water RO units, direct vapour generation (DVG) (Table 8) and heat transfer fluid (HTF) (Table 9) configuration of the solar power cycle and regenerative and non-

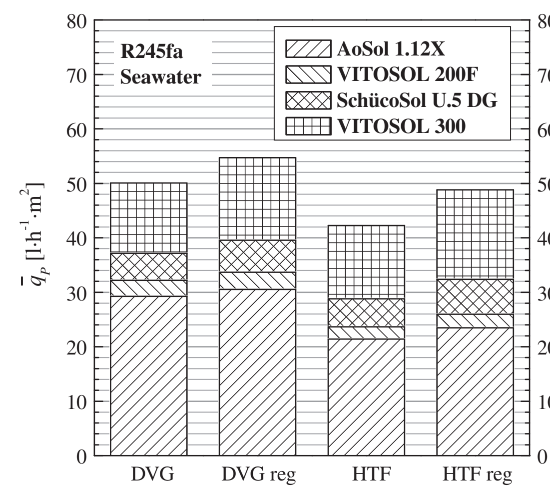

Fig. 8. Influence of solar cycle configuration over the unit volumetric flow rate of desalted water. Solar ORC with R245fa as working fluid and seawater at 20 °C as feed water of RO unit.

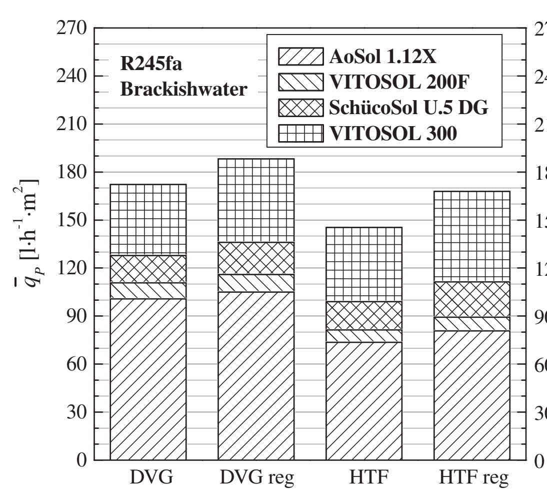

Fig. 9. Influence of solar cycle configuration over the unit volumetric flow rated of desalted water. Solar ORC with R245fa as working fluid and brackish water at 20 °C as feed water of RO unit.

regenerative organic Rankine cycle (ORC) with R245fa as working fluid.

Preheating of the feed water of desalination unit with the heat rejected by the solar cycle has been taken into account in the calculation of the values of unit volumetric flow rate of fresh water. Maximum temperature increase (7 °C) is attained with the lowest-efficiency solar cycle (non-regenerative HTF solar cycle with CPC AoSol 1.12X) and seawater RO unit. This temperature increase yields an increase of 1.9% in the volumetric flow rate of fresh water. Obviously, this value is higher than the obtained in the medium temperature solar thermal desalination system [11]. On the other hand, in the non-regenerative solar cycle starting heat rejection temperature values are between 50 °C and 60 °C except in the HTF configuration with FPC SchücoSol U.5 DG and ETC. VITOSOL 300. In the latter, heat rejection starts at temperatures between 70 °C and 80 °C. Two results related with the heating pressure of the ORC can be obtained from the data of Tables 8 and 9. On one hand, heating pressures in the HTF configuration are lower than in DVG configuration which is an expected result because there is a temperature drop in the heat exchanger matching the solar circuit and the ORC. On the other hand, heating pressures of the regenerative ORC are lower than in the non-regenerative one for the same configuration and solar collector. This result is even more interesting than the former because it means that the solar cycle with better efficiency due to the regeneration process has also a lower heating pressure.

Table 8
Main operation and design parameters of a reverse osmosis system driven by static solar collectors with a direct vapour generation (DVG) configuration of the solar ORC with R245fa as working fluid. $G = 1000\ W/m^2$, $T_{amb} = 25\ °C$.

Solar organic Rankine cycle (condensation temperature/pressure, 30 °C/177.8 kPa)								
Solar collector model	CPC Aosol 1.12X		FPC VITOSOL 200F		FPC SchücoSol U.5 DG		ETC. VITOSOL 300	
Recuperator effectiveness, ε_{reg}	0	0.8	0	0.8	0	0.8	0	0.8
Evaporation temperature, t_{evap} (°C)	100.0	98.0	100.0	95.0	113.0	108.0	148.0	137.0
Evaporation pressure, p_{evap} (kPa)	1264.6	1209.3	1264.6	1129.8	1671.3	1504.7	3273.9	2675.6
Cold stream temperature at recuperator's outlet, T_y (°C)	30.6	43.6	30.6	45.1	30.8	55.6	31.7	57.8
Superheating temperature, t_2 (°C)	100.0	100.0	100.0	100.0	113.0	125.0	150.0	150.0
Hot stream temperature at recuperator's outlet, T_x (°C)	51.4	35.1	51.4	35.6	54.6	39.4	58.4	40.6
Rankine cycle thermal efficiency, η_{ORC} (%)	11.12	11.81	11.12	11.59	12.24	13.63	14.22	16.07
Coupling with seawater reverse osmosis unit								
Working fluid mass flow rate, $\dot{m}$ (kg/s)	2.710	2.739	2.695	2.791	2.394	2.275	1.980	1.863
Thermal power rejected, $\dot{Q}_{x\to4}$ (kW)	563.8	526.6	563.8	538.0	505.6	447.0	425.4	368.2
Total solar collector aperture area, A_a (m^2)	1424.4	1365.8	1294.5	1237.2	1122.3	1053.8	832.8	762.0
Preheated seawater temperature, t_A (°C)	25.1	24.8	25.1	24.9	24.6	24.1	23.8	23.3
Unit volumetric flow rate, $\overline{q_p}$ (l h^{-1} m^{-2})	29.7	31.0	32.8	34.3	37.8	40.2	50.8	55.4
Coupling with brackish water reverse osmosis unit								
Working fluid mass flow rate, $\dot{m}$ (kg/s)	0.826	0.835	0.826	0.851	0.730	0.694	0.603	0.568
Thermal power rejected, $\dot{Q}_{x\to4}$ (kW)	171.8	160.5	171.8	164.0	154.1	136.2	129.7	112.2
Total solar collector aperture area, A_a (m^2)	434.1	416.3	394.5	377.1	342.0	321.2	253.8	232.2
Preheated brackish water temperature, t_A (°C)	22.0	21.9	22.0	21.9	21.8	21.6	21.5	21.3
Unit volumetric flow rate, $\overline{q_p}$ ((l/h)/m^2))	102.2	106.5	112.5	117.5	129.5	137.9	174.3	190.1

Table 9
Main operation and design parameters of a reverse osmosis system driven by static solar collectors with a heat transfer fluid (HTF) configuration of the solar ORC with R245fa as working fluid. $G = 1000\ W/m^2$, $T_{amb} = 25\ °C$.

Solar organic Rankine cycle (condensation temperature/pressure, 30 °C/177.8 kPa)								
Solar collector model	CPC Aosol 1.12X		FPC VITOSOL 200F		FPC SchücoSol U.5 DG		ETC. VITOSOL 300	
Recuperator effectiveness, ε_{reg}	0	0.8	0	0.8	0	0.8	0	0.8
Evaporation temperature, T_{evap} (°C)	83	82	83	82	100	100	130.0	124.0
Evaporation pressure, p_{evap} (kPa)	850.2	829.6	850.2	829.6	1264.6	1264.6	2344.2	2086.6
Cold stream temperature at recuperator's outlet, T_y (°C)	30.4	47.6	30.4	47.6	30.6	57.1	31.2	61.5
Superheating temperature, T_2 (°C)	95	95	95	95	117	122	145.0	145.0
Hot stream temperature at recuperator's outlet, T_x (°C)	59.7	36.4	59.7	36.4	71.4	39.9	78.5	41.7
ORC thermal efficiency, η_{ORC} (%)	9.28	10.14	9.28	10.14	11.12	12.88	13.54	15.46
HTF (water) inlet/outlet temperature (°C)	82.8/100	83.3/100	82.8/100	83.3/100	94.3/122	96.5/127	116.7/150	114.3/150
Coupling with seawater reverse osmosis unit								
Working fluid mass flow rate, $\dot{m}$ (kg/s)	3.55	3.57	3.55	3.57	2.616	2.526	1.993	2.000
Thermal power rejected, $\dot{Q}_{x\to4}$ (kW)	767.4	690.8	767.4	690.8	595.1	497.6	467.6	397.5
HTF (water) mass flow rate, $\dot{m}_{water}$ (kg/s)	11.55	10.85	11.55	10.85	5.686	4.407	3.787	3.071
Total solar collector aperture area, A_a (m^2)	1948.7	1775.8	1761.4	1605.5	1448.2	1288.2	986.8	854.2
Preheated seawater temperature, t_A (°C)	27.0	26.3	27.0	26.3	25.4	24.5	24.2	23.6
Unit volumetric flow rate, $\overline{q_p}$ (l h^{-1} m^{-2})	21.8	23.9	24.1	26.5	29.3	32.8	42.8	49.3
Coupling with brackish water reverse osmosis unit								
Working fluid mass flow rate, $\dot{m}$ (kg/s)	1.082	1.088	1.082	1.088	0.797	0.770	0.607	0.610
Thermal power rejected, $\dot{Q}_{x\to4}$ (kW)	233.9	210.5	233.9	210.5	181.4	151.6	142.5	121.2
HTF (water) mass flow rate, $\dot{m}_{water}$ (kg/s)	3.521	3.307	3.521	3.307	1.733	1.343	1.154	0.936
Total solar collector aperture area, A_a (m^2)	593.2	541.2	536.8	489.3	441.4	392.6	300.7	260.3
Preheated brackish water temperature, t_A (°C)	22.8	22.5	22.8	22.5	22.1	21.8	21.7	21.4
Unit volumetric flow rate, $\overline{q_p}$ (l h^{-1} m^{-2})	75.3	82.2	82.5	91.0	100.7	112.8	147.2	169.8

4. Conclusions

The performed analysis of seawater and brackish water reverse osmosis desalination driven by low-temperature solar organic Rankine cycle (ORC) yields the following conclusions.

For a solar irradiance of 1000 W/m^2 over the aperture area of the solar collector and a condensation temperature of 30 °C in the ORC, values of volumetric flow rate of desalted water per square meter of aperture area between 21 l h^{-1} m^{-2} and 31 l h^{-1} m^{-2} with CPC AoSol 1.12X, between 23 l h^{-1} m^{-2} and 40 l h^{-1} m^{-2} with FPC VITOSOL 200 and FPC SchücoSol U.5 DG and between 41 l h^{-1} m^{-2} and 51 l h^{-1} m^{-2} with ETC. VITOSOL 300 can be attained with a solar thermal driven seawater reverse osmosis unit. In the case of brackish water reverse osmosis, values are between 72 l h^{-1} m^{-2} and 108 l h^{-1} m^{-2} with CPC AoSol 1.12X, between 80 l h^{-1} m^{-2} and 138 l h^{-1} m^{-2} with FPC VITOSOL 200 and FPC SchücoSol U.5 DG and between 142 l h^{-1} m^{-2} and 198 l h^{-1} m^{-2} with ETC. VITOSOL 300. Values of unit volumetric flow rate decrease in approximately 0.5 l h^{-1} m^{-2} and 1.7 l h^{-1} m^{-2} in the case of seawater and brackish water RO, respectively per every degree of increasing in condensation temperature of the solar ORC with R245fa as working fluid. With this fluid, values of preliminary design parameters of the solar thermal driven reverse osmosis systems shows that the maximum increase in the productivity of the solar desalination systems is below 2% if the feed water is preheated with the thermal energy rejected by the solar ORC. In the non-regenerative preliminary designs proposed, heat rejection of thermal energy starts at temperatures between 50 °C and 80 °C so it should be analysed the use of this discarded thermal energy in applications different than preheating of the feed water of the RO unit.

Acknowledgements

The authors wish to thank the European Commission for its partially financial assistance within the International Cooperation Activities Programme ("POWERSOL" Project, Contract No. FP6-INCO2004-MPC3-032,344).

References

[1] [1] OSMOSOL project. <https://www.psa.es/webeng/projects/joomla/osmosol/>. [accessed 12.09.09].
[2] POWERSOL project. <https://www.psa.es/webeng/projects/joomla/powersol/>. [accessed 12.09.09].
[3] Delgado-Torres AM. Diseño preliminar de un sistema de desalación por ósmosis inversa mediante energía solar térmica. Academic thesis, Departamento de Física Fundamental y Experimental, Electrónica y Sistemas, Universidad de La Laguna; 2006. ISBN: 978-84-7756-740-0.
[4] Delgado-Torres AM, Garcia-Rodriguez L. Status of solar thermal-driven reverse osmosis desalination. Desalination 2007;216:242–51.
[5] Ghermandi A, Messalem R. Solar-driven desalination with reverse osmosis: the state of the art. Desalination Water Treat 2009;7:285–96.
[6] Manolakos D, Papadakis G, Mohamed ES, Kyritsis S, Bouzianas K. Design of an autonomous low-temperature solar rankine cycle system for reverse osmosis desalination. Desalination 2005;183:73–80.
[7] Manolakos D, Kosmadakis G, Kyritsis S, Papadakis G. On site experimental evaluation of a low-temperature solar organic rankine cycle system for RO desalination. Sol Energy 2009;83:646–56.
[8] Manolakos D, Papadakis G, Kyritsis S, Bouzianas K. Experimental evaluation of an autonomous low-temperature solar rankine cycle system for reverse osmosis desalination. Desalination 2007;203:366–74.
[9] Manolakos D, Kosmadakis G, Kyritsis S, Papadakis G. Identification of behaviour and evaluation of performance of small scale, low-temperature organic rankine cycle system coupled with a RO desalination unit. Energy 2009;34:767–74.
[10] Delgado-Torres AM. Solar thermal heat engines for water pumping: an update. Renew Sust Energy Rev 2009;13:462–72.
[11] Delgado-Torres AM, Garcia-Rodriguez L, Romero-Ternero VJ. Preliminary design of a solar thermal-powered seawater reverse osmosis system. Desalination 2007;216:292–305.
[12] Delgado-Torres AM, Garcia-Rodriguez L. Double cascade organic rankine cycle for solar-driven reverse osmosis desalination. Desalination 2007;216:306–13.
[13] Schuster A, Karellas S, Kakaras E, Spliethoff H. Energetic and economic investigation of organic rankine cycle applications. Appl Therm Eng 2009;29:1809–17.
[14] Kosmadakis G, Manolakos D, Kyritsis S, Papadakis G. Economic assessment of a two-stage solar organic Rankine cycle for reverse osmosis desalination. Renew Energy 2009;34:1579–86.
[15] Kosmadakis G, Manolakos D, Kyritsis S, Papadakis G. Simulation of an autonomous, two-stage solar organic Rankine cycle system for reverse osmosis desalination. Desalination Water Treat 2009;1:114–27.
[16] Bruno JC, Lopez-Villada J, Letelier E, Romera S, Coronas A. Modelling and optimisation of solar organic Rankine cycle engines for reverse osmosis desalination. Appl Therm Eng 2008;28:2212–26.
[17] Delgado-Torres AM, García-Rodríguez L. Analysis and optimization of the low-temperature solar organic rankine cycle (ORC). Energy Convers Manage; 2009 [unpublished results].
[18] Delgado-Torres AM, Garcia-Rodriguez L. Preliminary assessment of solar organic Rankine cycles for driving a desalination system. Desalination 2007;216:252–75.
[19] The solar key mark collector database. <http://solarkey.dk/solarkeymarkdata/CollectorCertificates/solarkeymarkCollectorCertificates.aspx>. [accessed 12.09.09].
[20] Bucker D, Wagner W. Reference equations of state for the thermodynamic properties of fluid phase n-butane and isobutane. J Phys Chem Ref Data 2006;35:929–1019.
[21] DuPont. <http://www2.dupont.com/Directories/en_US/Products_Services_Index/index.html>. [accessed 12.09.09].
[22] International chemical safety cards. <http://www.ilo.org/public/english/protection/safework/cis/products/icsc/>. [accessed 12.09.09].
[23] Federal register environmental documents. <http://www.epa.gov/EPA-AIR/>. [accessed 12.09.09].
[24] Lemmon EW, Span R. Short fundamental equations of state for 20 industrial fluids. J Chem Eng Data 2006;51:785–850.
[25] BOC GASES. safety data sheet. <http://www.bocsds.com/uk/sds/special/R245fa.pdf>. [accessed 12.09.09].
[26] World meteorological organization (WMO). Scientific assessment of ozone depletion: 2006. Global ozone research and monitoring project—report, Geneva, Switzerland; 2007.
[27] NIST chemistry webook. <http://webbook.nist.gov/chemistry/fluid/>. [accessed 12.09.09].
[28] Angelino G, Di Paliano PC. Multicomponent working fluids for organic rankine cycles (ORCs). Energy 1998;23:449–63.
[29] Quoilin S. Experimental study and modeling of a low temperature rankine cycle for small scale cogeneration. Academic thesis, Thermodynamics Laboratory, Aerospace and Mechanical Engineering Department, Faculty of Applied Sciences, University of Liege; 2007.
[30] Invernizzi C, Iora P, Silva P. Bottoming micro-Rankine cycles for micro-gas turbines. Appl Therm Eng 2007;27:100–10.
[31] Wilf M. The guidebook to membrane desalination technology: reverse osmosis, nanofiltration and hybrid systems, process, design, applications and economics. L'Aquila, Italy: Balaban Desalination Publications; 2007.
[32] García-Rodríguez L. Estudio termoeconómico de la desalación de agua de mar mediante colectores cilindroparabólicos. Academic thesis, Departamento de Física Fundamental y Experimental, Electrónica y Sistemas,Universidad de La Laguna;1999.